Journal of Photochemistry and Photobiology B: Biology 101 (2010) 313–320

Contents lists available at ScienceDirect

Journal of Photochemistry and Photobiology B: Biology

journal homepage: www.elsevier.com/locate/jphotobiol

Measuring bacterial growth by refractive index tapered fiber optic biosensor

Mohammad Ismail Zibaii [a], Alireza Kazemi [a], Hamid Latifi [a,*], Mahmoud Karimi Azar [b], Seyed Masoud Hosseini [b], Mohammad Hossein Ghezelaiagh [a]

[a] Laser & Plasma Research Institute, Shahid Beheshti University, Evin, Tehran, Iran
[b] Department of Microbiology, Faculty of Biological Sciences, Shahid Beheshti University, Evin, Tehran, Iran

ARTICLE INFO

Article history:
Received 15 March 2010
Received in revised form 1 July 2010
Accepted 30 July 2010
Available online 10 August 2010

Keywords:
Tapered fiber optic
Escherichia coli
Refractive index
Growth rate
Poly-L-Lysine

ABSTRACT

A single-mode tapered fiber optic biosensor was utilized for real-time monitoring of the *Escherichia coli* (*E. coli* K-12) growth in an aqueous medium. The applied fiber tapers were fabricated using heat-pulling method with waist diameter and length of 6–7 μm and 3 mm, respectively. The bacteria were immobilized on the tapered surface using Poly-L-Lysine. By providing the proper condition, bacterial population growth on the tapered surface increases the average surface density of the cells and consequently the refractive index (RI) of the tapered region would increase. The adsorption of the cells on the tapered fiber leads to changes in the optical characteristics of the taper. This affects the evanescent field leading to changes in optical throughput. The bacterial growth rate was monitored at room temperature by transmission of a 1558.17 nm distributed feedback (DFB) laser through the tapered fiber. At the same condition, after determining the growth rate of *E. coli* by means of colony counting method, we compared the results with that obtained from the fiber sensor measurements. This novel sensing method, promises new application such as rapid analysis of the presence of bacteria.

1. Introduction

1.1. Escherichia coli

Escherichia coli (*E. coli*) naturally exist in the intestinal tract of humans and warm-blooded animals. The bacterial genes are comparatively simple; therefore, these genes can be easily-manipulated or duplicated through a process of reproduction. A series of genetic manipulating systems have also been developed which allows the production of recombinant proteins using *E. coli*. One of the useful applications of recombinant DNA technology is in the production of human insulin [1], and moreover modified *E. coli* have been used in vaccine development, bioremediation and production of immobilized enzymes [2]. On the other hand, some of *E. coli* strains such as serotype O157:H7 can cause serious food poisoning in human, and are occasionally responsible for costly product recalls [3]. In view of the fact that, *E. coli* are not always confined to the intestine, their ability to survive for brief periods outside the body makes them an ideal microorganism to test environmental samples for fecal contamination. The positive and negative features of *E. coli* places them among the best-studied model organisms and one of the most important species in biotechnology and microbiology.

Measuring the growth rate of these bacteria has become an important issue in laboratories, food industry, and pharmaceutical companies. The effect of temperature variation and media composition on the growth rate of the bacteria has been studied extensively [4]. In the conventional methods, the contaminated sample is grown in an enriched medium for 6–18 h. Some other convenient and safe counting methods have led to the development of a number of sensors for real-time bioprocess monitoring of bacterial growth. These methods involve *in situ* monitoring systems which were developed for measuring dissolved oxygen [5,6], carbon-dioxide [7], optical density (OD) [8–11], heat exchange [12,13], and pH [5,6]. Several real-time bioprocess monitoring systems have been introduced including piezoelectric sensors [14,15], impedance spectroscopy measurement [16–19], and micromechanical oscillator [20] which are illustrated in Table 1.

Refractive index (RI) measurement in small volumes plays a vital role in many areas of biophysics, biochemistry and biomedicine. For instance, chemical or composition changes inside the cells can be measured by RI method [21], while the traditional bulk refractometers are not appropriate for such an application. Currently, the RI measurement method is a new and powerful way for determining the growth rate of living cells.

Fiber based RI sensors (FBRIS) are one of the RI measurement structures which represent several advantageous features such as small size, immunity from electromagnetic interference, corrosion resistance, and remote sensing capability. In addition, FBRISs could be easily multiplexed on a single fiber network. These characteristics give them preference over other techniques for biological applications.

* Corresponding author. Tel.: +98 2129902675; fax: +98 22431775.
E-mail address: latifi@cc.sbu.ac.ir (H. Latifi).

1011-1344/$ - see front matter © 2010 Elsevier B.V. All rights reserved.
doi:10.1016/j.jphotobiol.2010.07.017

Table 1
Comparison of various methods for monitoring bacterial growth rate.

Method	Sensor size	Measured parameter	Detection limit	Advantage	Disadvantage	Ref.
Dissolved oxygen (dO_2)	16.3 cm × 8.9 cm × 2.2 cm (sensor dish reader)	Dissolved oxygen in the growth medium (dO_2)	2% dO_2	Easy to predict cell growth owing to its low solubility	1. Need to fluorogenic compounds 2. The results will require interpretation, and are not as clear-cut as direct measurement	[5,6]
Dissolved CO_2 (dCO_2)	12 mm diameter × 320 mm insertion depth	Dissolved carbon-dioxide in the growth medium (dCO_2)	0.5% dCO_2	Easy to predict cell growth owing to a product of cell respiration	1. Problem with interference from changes in culture media composition 2. Expensive 3. Need to special calibrations	[7]
OD	1 cm square cuvette	Concentration of bacteria in a suspension ($g\,l^{-1}$)	3 $g\,l^{-1}$	1. Fast, not required pre-treatment 2. Relatively high signal-to-noise	1. Fault analysis of a high density *E. coli* unicellular process 2. Difficulty of calibration 3. The sensitivity is limited to about 10^7 cells per ml for most bacteria	[8–11]
Heat-exchange	Bench-scale calorimeters	Concentration of bacteria in the growth medium ($g\,l^{-1}$)	4.5 $g\,l^{-1}$	Cost effective and simple	1. Side effect such as heat loss 2. Data could be changed by broth composition and cell concentration	[12,13]
pH	16.3 cm × 8.9 cm × 2.2 cm (sensor dish reader)	Acidity of the growth medium (pH)	0.05 (pH)	Good reproducibility and durability	1. Need to fluorogenic compounds 2. The results will require interpretation, and are not as clear-cut as direct measurement	[5,6]
Piezoelectricity	Quartz crystals (13.7 mm diameter) with electrodes (5.1 mm diameter ×1000 A° thickness)	Cell density on the quartz crystal (cells ml^{-1})	10^3 cells ml^{-1}	1. Inexpensive 2. Suitable to be used in a disposable format	Need to immobilization of affinity-purified antibodies	[14,15]
Impedance spectroscopy	5–19 mm diameter and 25 mm long	Cell density in the growth medium (cells ml^{-1})	10^6 cells ml^{-1}	1. High signal-to-noise ratio 2. Inexpensive	1. Poor sensitivity 2. Problems of nonspecific binding 3.Low sensitivity under 10^6/ml cell concentration	[16–19]
Micromechanical oscillator	0.5 mm × 0.1 mm and 0.007 mm thickness	Strain in term of oscillation ($pg\,Hz^{-1}$)	140 $pg\,Hz^{-1}$	1. Rapid real-time detection 2. Label-free 3. Small analyte volume	1. Special configures are needed 2. Sensitive to additional mass loading onto the cantilever	[20]

FBRISs are classified into long period grating (LPG) [22–25], fiber Bragg grating (FBG) [26–28], hybrid LPG–FBG structures [29,30], metal coated fiber using surface Plasmon resonance [31,32], localized surface Plasmon [33], multi-mode tapered fiber (MMTF) [34], and single-mode tapered fiber (SMTF) [35]. Although these configurations were proposed as fiber sensors, there are still some limitations for the RI measurement. Some of the limitations and advantages of the mentioned approaches are summarized in Table 2.

Previous work in the bacterial growth rate was monitored by 480 nm light transmission through the tapered fiber [36] which showed that changes in transmission was a measure of change in

Table 2
Comparison of various refractive index measurement techniques using fiber optic sensors (detection limit is given in RI unit (RIU)).

Type	Measurement range (RIU)	Detection limit (RIU)	Advantage	Disadvantage	Ref.
Long period grating (LPG)	1.33–1.426	2.1×10^{-5}	If combined with other techniques (i.e. gold coated, Arc-induced phase shifted, asymmetric), high sensitivity for a large RI range	1. Needs special fiber and fabrication techniques 2. High cost 3. To sense RI, special configures are needed	[22,25]
Fiber Bragg grating (FBG)	Close to 1.333 Close to 1.450	10^{-4} 10^{-5}	If combined with other techniques (i.e. side polished, tapering, metal coated and gold coated), high sensitivity to detect RI	1. Needs special fiber and fabrication techniques 2. High cost 3. To sense RI, special configures are needed	[26–28]
Hybrid LPG–FBG	1.33–1.40 1.42–144	1.4×10^{-4} 2×10^{-5}	High sensitivity to detect RI	1. Complicated design 2. High cost 3. Instable system	[29,30]
Surface Plasmon resonance	Close to 1.333 Close to 1.398	2.1×10^{-4} 1.5×10^{-4}	High sensitivity to detect RI	1. Needs special fabrication techniques 2. High cost	[31,32]
Localized surface Plasmon resonance	1.33–1.35	3.8×10^{-5}	High sensitivity for the RI	1. Needs special fabrication techniques 2. Needs immobilization of gold nanoparticles 3. High cost	[33]
Multi-mode tapered fiber (MMTF)	1.36–1.46	$<10^{-4}$	1. Low fabrication cost 2. High sensitivity for the RI close to cladding RI	Low sensitivity for RI from 1.3 to 1.4	[34]
Single-mode tapered fiber (SMTF)	1.333–1.350	1.4×10^{-5}	1. Low fabrication cost 2. High sensitivity for the RI	Fragile and hard to clean	[35]

absorption of the evanescent field (EVF). In this study the bacterial growth rate was monitored by transmission of a 1558.17 nm distributed feedback (DFB) laser through the tapered fiber which studies the effect of bacterial growth on RI and laser radiation effect on bacterial growth rate were investigated. RI variation was calculated by measuring bacterial growth rate and RI model for cell which used in Ref. [37]. Our sensor is believed to demonstrate modestly enhanced sensitivity and the simplicity of design compared to other previous sensor [37].

The aim of this study is to fabricate a RI tapered fiber optic biosensor (TFOBS) in order to determine the growth rate of *E. coli* K-12 at room temperature which is useful in measuring the bacterial contamination in food industries.

2. Physics of tapered fiber optic

Traditionally, optical fibers are cylindrical waveguides with an inner core of Ge-doped silica surrounded by a cladding of pure silica. Physical characteristics of the fiber such as the refractive index, core diameter and the operating wavelength determine the number and type of the modes propagating through the fiber. The main portion of the light energy is carried into the core and only a minute portion penetrates into the clad. The latter portion decays exponentially into the core–cladding boundary that is known as EVF. The penetration depth of EVF in an intact fiber is given by [38]:

$$d_p = \frac{\lambda}{2\pi\sqrt{n_{co}^2 \sin^2\theta_{\text{int}} - n_{cl}^2}} \quad (1)$$

where θ_{int} is the incident angle at the core/cladding interface.

The number of modes which can be supported in the fiber is described by *V*-number:

$$V_{co} = \frac{2\pi a}{\lambda}\sqrt{n_{co}^2 - n_{cl}^2} \quad (2)$$

where a, λ, n_{co}, and n_{cl} are the radius of the core, wavelength of a source, cladding, and core RIs, respectively. When a single-mode optical fiber is tapered, the core *V*-number decreases ($V_{co} < 1$) as a result of the reduction in the fiber radius. On the other hand, the cladding *V*-number increases ($V_{cl} > 2.405$) from the difference in RI between the cladding and the sample. As $V_{co} < 1$, the light is no longer guided by the core–cladding boundary. Therefore, the core/cladding interface is redefined in such a way that the light propagation inside the core spreads to the cladding, which plays the role of the new core, and the external medium is now the new cladding [38,39]. The new *V*-number is called V_{cl} is given by:

$$V_{cl}(z) = \frac{2\pi a(z)}{\lambda}\sqrt{n_{cl}^2 - n_{ex}^2} \quad (3)$$

where $a(z)$ and n_{ex} are the radius of the fiber in the $V_{co} < 1$ region and the RI of the external medium, respectively. Thus, the effect of tapering is to create a region, where cladding modes exist and thus support many modes. The tapering acts as a perturbation mechanism resulting in coupling among the modes that can be supported due to the high value of $V_{cl}(z)$ [39,40]. The penetration depth then depends on the RI of the external medium surrounding the taper (n_{ex}) and the incident angle (θ_{int}) at the core/cladding interface, and is given by [41]:

$$d_p = \frac{\lambda}{2\pi\sqrt{n_{cl}^2 \sin^2\theta_{\text{int}} - n_{ex}^2}} \quad (4)$$

In the sensors applications, the RI of the aqueous sample is typically 1.33, and that of the original core and cladding are 1.485 and 1.460, respectively. Thus, the practical EVF penetration depth for sensing at 1558.17 nm (used in this study) is calculated to be approximately 0.42 μm. Assuming that the bacterial cells are about 1–2 μm, the EVF depth is enough to interact with target cells in aqueous solutions.

On the other hand, amplitude of the EVF is typically very low in a normal single-mode fiber, but it can be enhanced significantly by tapering [42]. Because of the departure from cylindrical symmetry, tapering of a single-mode fiber necessarily couples power from the fundamental mode into the higher-order modes. This perturbation mechanism increases the EVF amplitude and thereby the interaction of the transmitted light with the analyte lying on the taper is enhanced [39,40,43].

With the growth of the bacteria on the tapered region, changes in the RI of the clad leads to changes in optical throughput [38,44–47]. As a result, bacterial growth will cause a corresponding change in the transmitted light. By measuring the transmitted light variations, determination of the related bacterial surface concentration would be feasible.

3. Materials and methods

3.1. Tapered fiber fabrication

Fig. 1a illustrates the heat-pulling system using a CO_2 laser to fabricate tapered optical fiber. The CO_2 laser beam (SYNARD, 48–1SAL, 30w full power) focused via a Zn–Se lens of 2.5 cm focal length. The resultant spot size is about 120 μm on the fiber length. One end of the fiber was fixed on a translation stage and the other end was attached to a 5.12 g weight so that the fiber was subject to a constant tension during laser irradiation. The value of utilized weight has been optimized to fabricate tapers with desired structures. Fig. 1b shows one of the typical fabricated tapered fibers. A microscope was employed to monitor the tapering process. To measure the transmission characteristics of the fabricated tapered fiber, light from a wide bandwidth source was launched into the taper via a short SMF pigtail as shown in Fig. 1a. The output power from the tapered fiber was observed by an optical spectrum analyzer (OSA). The geometric characteristic of the fabricated taper depends on the power, number of pulses, beam shape, and duty cycle of the CO_2 laser. The exerted strain due to the 5.12 g attached weight and the focusing optics both affect the geometry of the tapered fiber.

3.2. Experimental set up

The experimental set up is shown in Fig. 2a. It consists of a DFB laser (Anritsu D54035) with maximum rated output power of 20 mW and peak wavelength of 1558.17 nm. In all the experiments, DFB laser was operated at 50 μW output power. The laser beam which arrives at the tapered fiber sensor after passing a dual stage isolator and a 2×2 coupler, is detected by photodiode 2 (PD2) which is called I_{sig}. The reflected light of the coupler is then observed by photodiode 1 (PD1) and is labeled as reference beam (I_{ref}). Finally, the data obtained from the two identical detectors is delivered to an A/D converter and is observed by Labview software. Measurement range of the optical detector is from 0.05 μW to 5 μW. The experimental indicator which specifies the RI of the liquid under test is defined as:

$$S = \frac{I_{sig}}{I_{ref}} \quad (5)$$

3.3. Fiber holder

As it can be seen in Fig. 2b, a microbioreactor is made of a thick Plexiglass to keep the tapered fiber in contact with liquid materials

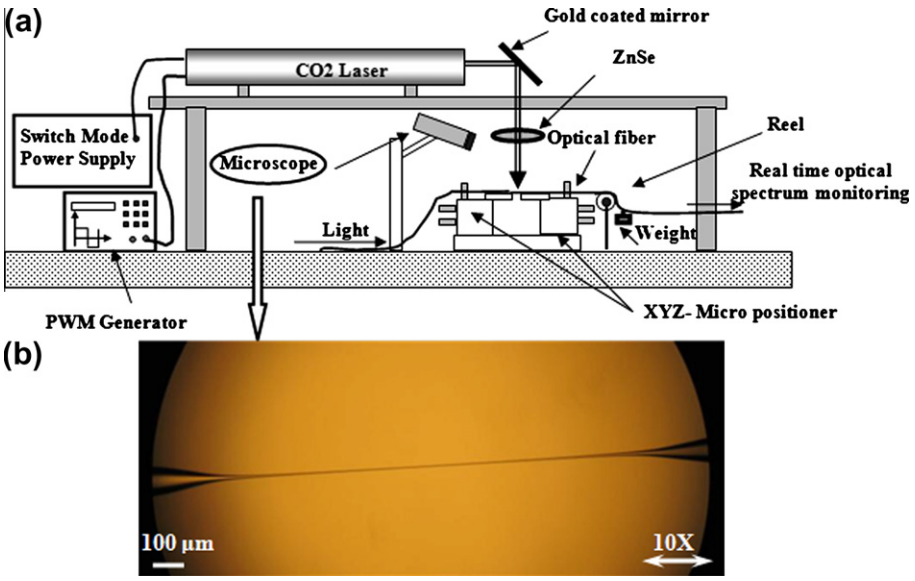

Fig. 1. (a) The fabrication system and (b) photograph of a tapered fiber fabricated in this study.

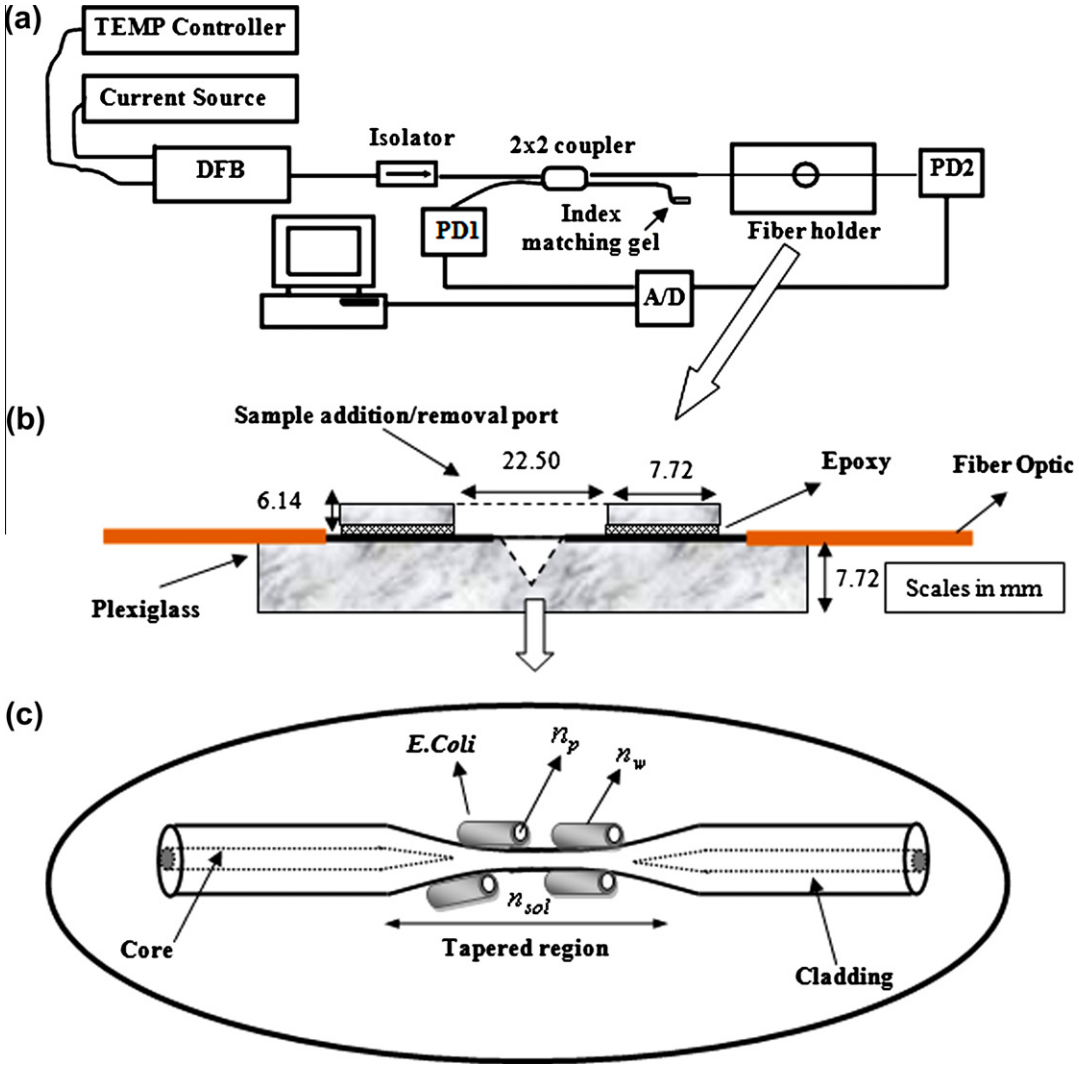

Fig. 2. (a) Instrumentation set up of a real-time monitored bacterial growth rate; (b) schematic of microbioreactor design; and (c) schematic of immobilization of rod like *E. coli* bacteria bound with their axis aligned parallel to the surface but otherwise at arbitrary orientation. n_w, n_p, and n_{sol} are the refractive indices of the bacteria cell wall, protoplasm of the bacteria and the surrounding aqueous solution, respectively.

like Poly-L-Lysine (PLL), bacteria, and culture mediums used in various experiments. The taper was fixed using epoxy (HIGH-TEMP RTV Silicone) between two pieces of Plexiglass. A 5 mm conical hole was drilled in Plexiglass, and a line was scored across the microwell with a CO_2 laser to accommodate the tapered fiber. Another Plexiglas was placed on the top, close to the microwell. The fabricated microwell has a 700–800 μl sample volume.

3.4. Tapered fiber immobilizations

PLL is commonly used to immobilize negatively charged molecules such as bacteria and DNA to glass surfaces. This substance includes positively charged amino-groups which can bind to a negatively charged silica surface through an ionic binding [48]. To immobilize *E. coli* on the sensing area, the tapered section of each fiber was washed with 70% ethanol (v/v) containing 1% HCl (v/v), then rinsed with deionized water at room temperature. The fiber was dried in microbiological safety cabinet for 30 min. Each taper fiber was overwhelmed by PLL solution of 0.1% PLL (Sigma, P8920) and was allowed to evaporate over night.

3.5. Bacteria and culture method

E. coli K-12 was grown under optimal conditions in Nutrient Broth (Merck) at 37 °C. A 14–18-h culture was used for experimental purposes to mimic environmental conditions. The cell suspension was centrifuged (Sigma, 3k30, 845g, 5 min, 4 °C) and the supernatant removed. The pellet was resuspended in sterile phosphate-buffered saline-A (PBS-A) to obtain an *E. coli* concentration of approximately 10^8 colony-forming units (CFU)/ml as determined by 0.5 McFarland standard and spectrophotometric assays. Typical growth experiment was conducted by non-colored growth medium (PBS-A, yeast extract (0.1 g/l) and glucose (1 g/l)) (Merck) inoculating 10^8 (CFU)/ml of *E. coli*.

3.6. Fiber sensor growth rate measurement

The first step was to determine the response of the sensor to the growth medium. The growth medium was added to the sensor holder and the background output of the sensor is measured for several hours. In the second step, after removing the growth medium from the fiber holder, the bacteria diluted in PBS-A was added to the sensor holder, so that the cells have contact with the coated taper for 30 min. By washing the holder with PBS-A, the unattached cells were removed and the growth medium was added to the holder again. The transmitted intensity of the sensor was again monitored for several hours.

3.7. Pour plate method for growth rate measurement

The growth rate of the bacteria must be determined in the same condition via colony counting method in order to examine the fiber sensor measurements. At first, 1 ml of the bacterial solution was added to the 250 ml glucose growth medium (GGM) which is labeled as sample flask. Using a sterile pipette tip, 0.1 ml of sample flask was removed every 30 min to prepare low concentration bacterial solutions (diluted serials: 10^{-1}–10^{-8} cells ml^{-1}). The mentioned procedure is called serial dilutions of bacteria in GGM. In the next step, 0.1 ml of each of the diluted serials was transferred to appropriate Casein-peptone Soymeal-peptone Agar (CASO Agar) plates. All CASO Agar plates were placed in the incubator at 37 °C for 48 h. In order to increase the accuracy of the counting, only the plates including with 10–30 colonies have been considered for calculation.

4. Result and discussion

4.1. Growth rate measurement with fiber optic

The output power of a tapered fiber can be written as

$$I = \alpha X^{\beta} \tag{6}$$

where X is the surface concentration per unit area, and α and β depend on the taper characteristics, as well as, optical properties of the *E. coli* which is grown on the taper [36]. During the exponential growth phase, a bacterial culture mimics a first-order chemical reaction, i.e. the rate of increase of the cells is proportional to the number of existing bacteria. The constant of proportionality, μ, is an index of the growth rate that can be determined from:

$$\ln\left(\frac{X}{X_0}\right) = \mu(t - t_0) \tag{7}$$

where X and X_0 are the concentration of cells at t and t_0, respectively. With changing of RI with time due to bacterial growth, the output intensity of through the tapered fiber also changes with time. In this case, the following analysis is valid as long as the time lag is constant; From Eq. (6), one can obtain:

$$\ln\left(\frac{I}{I_0}\right) = \beta \ln\left(\frac{X}{X_0}\right) \tag{8}$$

where, I_0 is the output power at the initial time. For a constant growth rate, Eq. (8) can be written as:

$$\ln\left(\frac{I}{I_0}\right) = \beta\mu t \tag{9}$$

Eq. (9) points out that the plot of $\ln(I/I_0)$ versus time will propose a straight line with the slope proportional to specific growth rate.

At the first step of growth rate measurement, where the tapered fiber is surrounded by the growth medium as described in Section 3.6, the background response of the sensor is determined by plotting the output intensity versus time as shown in Fig. 3. The calculated slope is 0.10 h^{-1}. In the second step of growth rate measurement during *E. coli* growth on the tapered fiber, the transmitted intensity of the sensor is plotted versus time in Fig. 4. The line slope called $\beta\mu$ is equal to -0.17 ± 0.01 h^{-1}. The negative slope

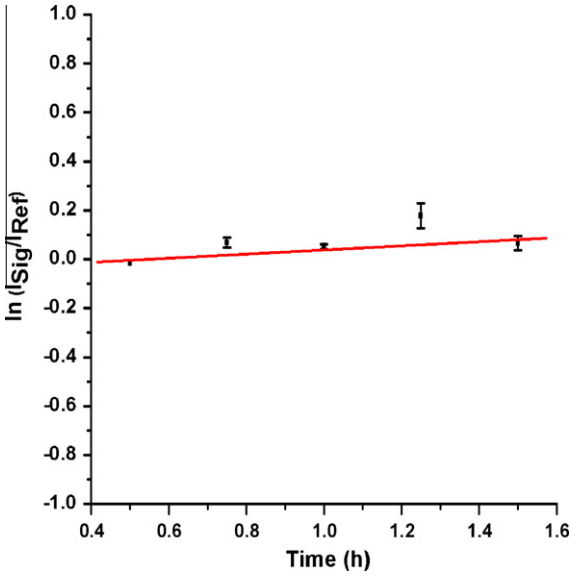

Fig. 3. Plot of sensor response versus time when the taper is surrounded by the growth medium in order to determine the background signal of the sensor (the bars are indicating the upper and lower limits of the repeated measurements).

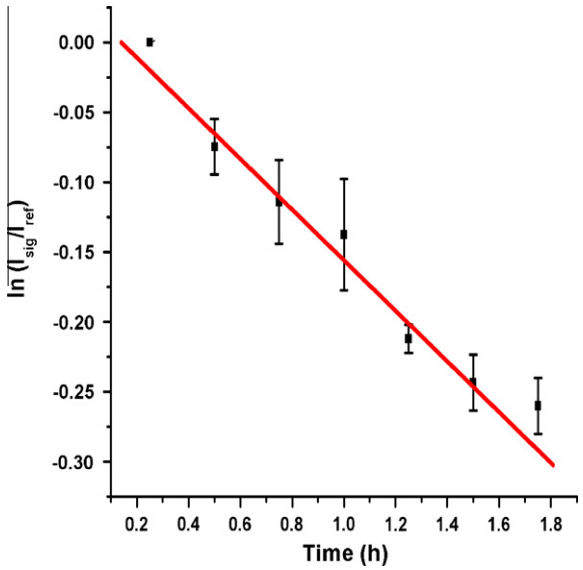

Fig. 4. Plot of sensor response versus time during *E. coli* growth on the tapered fiber. The culture was grown on a medium containing glucose and 0.1% yeast extract in PBS-A.

in Fig. 4, is three times lower than the slope of the Fig. 3, which demonstrates that during the bacterial growth, the transmitted intensity of the taper is decreased due to an increase in surface concentration. In a parallel experiment, the cells were grown on the same medium as described in Section 3.7. Log plot of cell number ratio is plotted as a function of time (Fig. 5) to determine the growth rate which is obtained to be $0.33 \pm 0.02\ h^{-1}$. The value of β determined from the slope in Fig. 4 is found to be -0.5, suggesting that this coefficient which characterizes the cell concentration in Eq. (6), is a constant.

4.2. The effect of bacterial growth on RI

The dielectric constant of the biological medium is described by [37]:

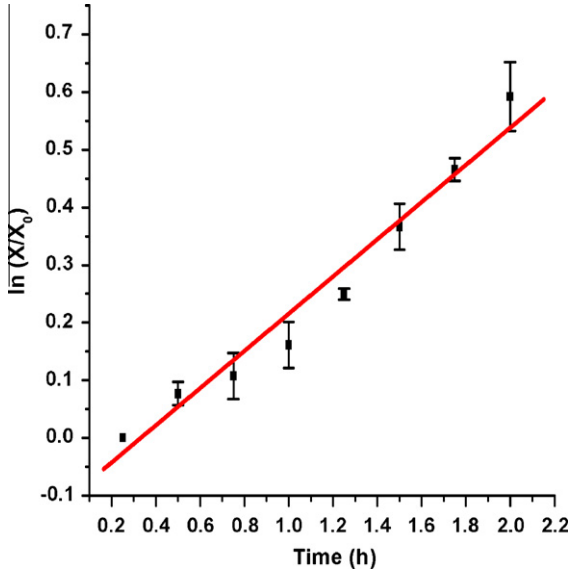

Fig. 5. Plot of *E. coli* concentration as a function of time. Culture was grown on a medium containing glucose and 0.1% yeast extract in PBS-A. Sample taken every 15 min were counted by pour plate method.

$$\varepsilon(r) = \varepsilon_{background} + \delta\varepsilon \tag{10}$$

where $\varepsilon_{background}$ is the dielectric constant of the background medium and $\delta\varepsilon$ indicates the variation of ε caused by bacteria growth. The schematic of immobilized bacteria on the surface of the taper has been shown in Fig. 2c. For a typical bacteria cell, let n_w and n_p be the RIs of the cell wall and protoplasm, respectively. Then it can be shown that [37]:

$$\delta\varepsilon = \sigma[(n_w^2 - n_{sol}^2)A + (n_p^2 - n_w^2)A'] \tag{11}$$

where A (A') is the average projection cross sectional area of the outer (inner) surfaces of the cell on the tapered surface and σ is the average surface density of the cells. Using a convergent length of 265.5 μm, waist diameter of 7 μm, waist length of 3080 μm, and divergent length of 248.5 μm, the taper surface was roughly calculated to be $17 \times 10^{-2}\ mm^2$. σ is determined by counting the number of bacteria (typically less than 200 counts) identified in the projected surface of $5.4 \times 10^{-2}\ mm^2$, which is only a fraction of the total taper surface. At the beginning of the experiment, the average surface density of the bacteria is about 3×10^3 *E. coli* mm^{-2}, which corresponds to an area occupied by approximately 155 bacteria. The total number of bacteria covered on the taper surface was measured via an optical microscope.

Resolution of the optical detectors in Fig. 2 is 0.05 μW which corresponds to a detection limit of 60 *E. coli* mm^{-2}. Considering the total area of the taper ($17 \times 10^{-2}\ mm^2$), we have a detection limit of 10 bacteria. The average weight of the *E. coli* bacteria is 2.8×10^{-13} g, which corresponds to sensitivity for bacteria dry-mass loading $17 \times 10^{-12}\ g\ mm^{-2}$.

For analysis purposes, the *E. coli* was modeled as a cylindrical cell with a rectangular contact area lying on taper wall. The model can be represented with the following parameters: *E. coli* cylinder radius ($b = 0.4$ μm) and cylinder half length ($a = 1$ μm) corresponds to an average *E. coli* volume about 1 μm^3. The cell wall thickness is estimated at $a - a' = b - b' = 42$ nm, RI of the bacteria cell wall ($n_w = 1.42$), and protoplasm of the bacteria ($n_p = 1.355$), which results in the average refractive index of $n \approx 1.37$ associated with *E. coli* and $n_{sol} = 1.33$ of the surrounding aqueous solution [37,49,50]. The presented RIs are associated with a $\lambda = 1.311$ μm central wavelength. The effective footprint of cylindrical area projection was found to be $2a \times 2b = 2\ \mu m \times 0.8\ \mu m$.

It is estimated that it would require 10^5 cells to completely cover the taper surface which means 155 cells cover <0.2% of the taper surface. According to Eq. (9), the change in RI was observed to be about 1.2×10^{-4} immediately after immobilizing *E. coli* on the taper. After initial immobilization, the growth of *E. coli* lying on the taper surface results in an average increase in the surface density of the cells and consequently an increase in the RI value of the taper cladding. Due to the presence of PLL on the taper, it is postulated that the added cells are immobilized on the taper surface via electrostatic absorption [36,37]. Using colony counting method, it was found out that the bacterial surface density increased from 3×10^3 *E. coli* mm^2 to 5×10^3 *E. coli* mm^2 in 1.6 h. The corresponding change in RI was 7×10^{-4}. Considering that in several growth experiments, the same reduction in transmission occurred, it is reasonable to conclude that the reduction in transmission was due to an increase in RI of the taper induced by increase in bacterial surface concentration.

4.3. Investigation of possible laser radiation effect on bacterial growth rate

As shown in Fig. 6, a controlled experiment was designed to investigate the effect of laser radiation on bacterial growth rate using the same laser source which had been used in the sensing experiments. The bacteria diluted in broth culture were prepared

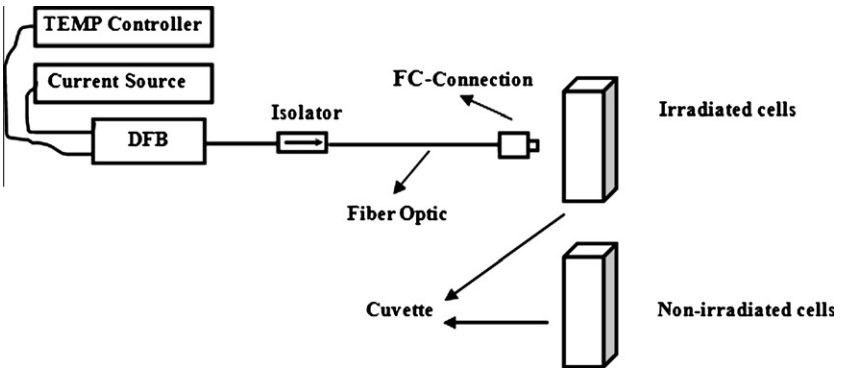

Fig. 6. Experimental set up of a controlled experiment to investigate the effect of laser radiation on bacterial growth rate.

in Nutrient Broth (Merck). It was then diluted so that turbidity equivalent to McFarland standard 0.5. From this diluted solution, 300 μl of bacterial culture was pipetted out and divided equally into two sterilized cuvettes of 1 cm optical path each of which contained 700 μl of GGM. Subsequent to 4 h exposure to the laser irradiation, 100 μl irradiated (experimental) and non-irradiated (control) cells were cultured on CASO Agar media (Merck). The number of colonies (CFU), were determined by pour plate method. No significant difference was found in survival of the bacterial cell count of the experimental group in comparison with the control group. The observation demonstrates that the laser radiation in the certain wavelength and output power has no direct side effect on the bacterial behavior.

5. Conclusion

In this article the use of a tapered fiber optic sensing device for *in situ* real-time monitoring of bacterial growth was demonstrated. The radius and length of the fiber sensor were 6–7 μm and 3 mm, respectively. The measured specific growth rate by tapered fiber optic biosensor and pour plate method were found to be $-0.17 \pm 0.01\ h^{-1}$ and $0.33 \pm 0.02\ h^{-1}$, respectively for 1.6 h period at room temperature. When the bacteria were grown on the taper, the fiber optic biosensor exhibited strong transmission changes at 1558 nm, which is proportional to the variation in cell concentration. Therefore, it can be inferred that the transmission through the fiber is decreased by an increase in the average surface density of the cells on the tapered fiber. The increase in the average density of the bacteria changes the dielectric constant of the new cladding (*E. coli* in the GGM) and the RI of the tapered section, as well. The sensitivity of the current set up is measured to be 60 *E. coli* mm^{-2}, which corresponds to 17×10^{-12} g mm^{-2} dry-mass loading or a total of 10 bacteria bound to the tapered surface. The new bacterial growth measurement system provides numerous advantages such as small size, rapid real-time, and label-free performance intended for small analyte volumes over other methods like plate counting, optical density, and dry weight.

References

[1] P. Feng, S. Weagant, M. Grant, Enumeration of *Escherichia coli* and the coliform bacteria. Bacteriological Analytical Manual, eighth ed. FDA/Center for Food Safety & Applied Nutrition, 2002.
[2] P. Cornelis, Expressing genes in different *Escherichia coli* compartments, Curr. Opin. Biotechnol. 11 (5) (2000) 450–454.
[3] R.L. Vogt, L. Dippold, *Escherichia coli* O157:H7 outbreak associated with consumption of ground beef, June–July 2002, Public Health Rep. 120 (2) (2005) 174–178.
[4] T. Ross, D.A. Ratkowsky, L.A. Mellefont, T.A. McMeekin, Modelling the effects of temperature, water activity, pH and lactic acid concentration on the growth rate of *Escherichia coli*, Int. J. Food Microbiol. 82 (2003) 33–43.
[5] K. Schneider, V. Schutz, G.T. John, E. Heinzle, Optical device for parallel online measurement of dissolved oxygen and pH in shake flask cultures, Bioprocess Biosyst. Eng. 6 (2009) 5, doi:10.1007/s00449-009-0367-0.
[6] M. Naciri, D. Kuystermans, M. Al-Rubeai, Monitoring pH and dissolved oxygen in mammalian cell culture using optical sensors, Cytotechnology 57 (2008) 245–250.
[7] R.N. Pattison, J. Swamy, B. Mendenhall, C. Hwang, B.T. Frohlich, Measurement and control of dissolved carbon dioxide in mammalian cell culture processes using an in situ fiber optic chemical sensor, Biotechnol. Prog. 16 (2000) 769–774.
[8] R. Thatipamala, S. Rohani, G. Hill, On-line monitoring of a wide range of biomass concentrations based on a new equation using a spectrophotometer: process control applications, J. Biotechnol. 38 (1994) 33–42.
[9] S.A. Arnolda, J. Crowley, S. Vaidyanathan, L. Matheson, P. Mohan, J.W. Hall, L.M. Harvey, B. McNeil, At-line monitoring of a submerged filamentous bacterial cultivation using near-infrared spectroscopy, Enzyme Microb. Technol. 27 (2000) 691–697.
[10] S. Vaidyanathan, A. Arnold, L. Matheson, P. Mohan, G. Macaloney, B. McNeil, L.M. Harvey, Critical evaluation of models developed for monitoring an industrial submerged bioprocess for antibiotic production using near-infrared spectroscopy, Biotechnol. Prog. 16 (2000) 1098–1105.
[11] V. Vojinovic, J.M.S. Cabral, L.P. Fonseca, Real-time bioprocess monitoring. Part I. In situ sensors, Sens. Actuators, B: Chem. 114 (2006) 1083–1091.
[12] U. Vonstockar, P. Duboc, L. Menoud, I.W. Marison, On-line calorimetry as a technique for process monitoring and control in biotechnology, Thermochim. Acta 300 (1997) 225–236.
[13] D. Voisard, U. V Stockar, I.W. Marison, Quantitative calorimetric investigation of fed-batch cultures of *Bacillus sphaericus* 1593M, Thermochim. Acta 394 (2002) 99–111.
[14] Y. Ishimori, I. Karube, S. Suzuki, Determination of microbial populations with piezoelectric membranes, Appl. Environ. Microbiol. 42 (1981) 632–637.
[15] X.-L. Su, Y. Li, A self-assembled monolayer-based piezoelectric immunosensor for rapid detection of *Escherichia coli* O157:H7, Biosens. Bioelectron. 19 (2004) 563–574.
[16] A.P. Ferreira, L.M. Vieira, J.P. Cardoso, J.C. Menezes, Evaluation of a new annular capacitance probe for biomass monitoring in industrial pilot-scale fermentations, J. Biotechnol. 116 (2005) 403–409.
[17] J.G. Guan, Y.Q. Miao, Q.J. Zhang, Impedimetric biosensors, J. Biosci. Bioeng. 97 (2004) 219–226.
[18] Y.H. Kim, J.S. Park, H. L Jung, An impedimetric biosensor for real-time monitoring of bacterial growth in a microbial fermentor, Sens. Actuators, B 138 (2009) 270–277.
[19] K. Mishima, A. Mimura, Y. Takahara, On-line monitoring of cell concentrations during yeast cultivation by dielectric measurements, J. Ferment. Bioeng. 72 (1991) 296–299.
[20] K.Y. Gfeller, N. Nugaeva, M. Hegner, Micromechanical oscillators as rapid biosensor for the detection of active growth of *Escherichia coli*, Biosens. Bioelectron. 21 (2005) 528–533.
[21] X.J. Liang, A.Q. Liu, X.M. Zhang, P.H. Yap, T.C. Ayi, H.S. Yoon, Determining refractive index of single living cell using an integrated microchip, Sens. Actuators, A 133 (2007) 349–354.
[22] J.H. Chong, P. Shum, H. Haryono, A. Yohana, M.K. Rao, C. Lu, Y. Zhu, Measurements of refractive index sensitivity using long-period grating refractometer, Opt. Commun. 229 (2004) 65–69.
[23] I.M. Ishaq, A. Quintela, S.W. James, G.J. Ashwell, J.M. Lopez-Higuera, R.P. Tatam, Modification of the refractive index response of long period gratings using thin film overlays, Sens. Actuators, B 107 (2005) 738–741.
[24] L.J. Tang, S.F. Cheng, W.T. Hsu, T.Y. Chiang, L.K. Chau, Fiber-optic biochemical sensing with a colloidal gold-modified long period fiber grating, Sens. Actuators, B 119 (2006) 105–109.
[25] J. Yang, L. Yang, C.Q. Xu, C. Xu, W. Huang, Y. Li, Long-period grating refractive index sensor with a modified cladding structure for large operational range and high sensitivity, Appl. Opt. 45 (2006) 6142–6147.

[26] A. Iadicicco, A. Cusano, A. Cutolo, R. Bernini, M. Giordano, Thinned fiber Bragg gratings as high sensitivity refractive index sensor, J. IEEE Photon. Technol. Lett. 16 (2004) 1149–1151.
[27] X. Shu, A.L.G. Bashir, Y. Liu, L. Zhang, I. Bennion, Sampled fiber Bragg grating for simultaneous refractive index and temperature measurement, Opt. Lett. 26 (2001) 774–776.
[28] K. Schroeder, W. Ecke, R. Mueller, R. Willsch, A. Andreev, A fiber Bragg grating refractometer, J. Meas. Sci. Technol. 12 (2001) 757–764.
[29] X. Chen, K. Zhou, L. Zhang, I. Bennion, Simultaneous measurement of temperature and external refractive index by use of a hybrid grating in D fiber with enhanced sensitivity by HF etching, Appl. Opt. 44 (2005) 178–182.
[30] A.P. Zhang, L.Y. Shao, J. F Ding, S. He, Sandwiched long-period gratings for simultaneous measurement of refractive index and temperature, J. IEEE Photon. Technol. Lett. 17 (2005) 2397.
[31] M. Iga, A. Seki, K. Watanabe, Hetero-core structured fiber optic surface Plasmon resonance sensor with silver film, Sens. Actuators, B 101 (2004) 368–372.
[32] D. Monzoon-Hernandez, V. Joel, D. Talavera, D. Luna-Moreno, Optical-fiber surface-Plasmon resonance sensor with multiple resonance peaks, Appl. Opt. 43 (2004) 1216–1220.
[33] V.V.R. Sai, T. Kundu, S. Mukherji, Novel U-bent fiber optic probe for localized surface Plasmon resonance based biosensor, Biosens. Bioelectron. 24 (2009) 2804–2809.
[34] J. Villatoro, D. Monzon-Hernandez, D. Talavera, High resolution refractive index sensing with cladded multimode tapered optical fiber, J. IEEE 40 (2004) 2.
[35] K. Quoc Kieu, M. Mansuripur, Biconical fiber taper sensor, J. IEEE Photon. 18 (21) (2006) 2239–2241.
[36] D. Maraldo, P.M. Shankar, R. Mutharasan, Measuring bacterial growth by tapered fiber and changes in evanescent field, Biosens. Bioelectron. 21 (7) (2006) 1339–1344.
[37] H.C. Ren, F. Vollmer, S. Arnold, A. Libchaber, High-Q microsphere biosensor analysis for adsorption of rodlike bacteria, Opt. Express 15 (25) (2007) 17410–17423.
[38] L.C. Bobb, P.M. Shankar, H.D. Krumboltz, Bending effects in biconically tapered single-mode fibers, J. Light Wave Technol. 8 (7) (1990) 1084–1090.
[39] A.W. Snyder, J.D. Love, Optical Waveguide Theory, Springer, Berlin, 1983.
[40] W.J. Stewart, J.D. Love, Design limitation on tapers and couplers in single-mode fibre tapers, Proc. ECOC 85 (1985) 559–562.
[41] M. Ahmad, L.L. Hench, Effect of taper geometries and launch angle on evanescent wave penetrations depth in optical fibers, Biosens. Bioelectron. 20 (2005) 1312–1319.
[42] A.G. Mignani, R. Falcial, L. Ciaccheri, Evanescent wave absorption spectroscopy by means of bi-tapered multimode optical fibers, Appl. Spectrosc. 52 (1998) 546–551.
[43] J.D. Love, W.M. Henry, Quantifying loss minimisation in single-mode fibre tapers, Electron. Lett. 22 (1986) 912–914.
[44] N. Nath, S. Anand, Evanescent wave fiber optic fluorosensor: effect of tapering configuration on the signal acquisition, Opt. Eng. 37 (1) (1998) 220–228.
[45] A.C. Boucouvalas, G. Georgiou, External refractive-index response of tapered coaxial couplers, Opt. Lett. 11 (1986) 257–259.
[46] J. Bures, R. Ghosh, Power density of the evanescent field in the vicinity of a tapered fiber, J. Opt. Soc. Am. A 16 (1999) 1992–1996.
[47] J. Voros, The density and refractive index of adsorbing protein layers, Biophys. J. 87 (2004) 553–561.
[48] G.T. Hermanson, Bioconjugate Techniques, Elsevier, San Diego, 1996.
[49] M. Ardhammer, P. Lincoln, B. Norden, In visible leptosomes: refractive index matching with sucrose enables flow dichroism assessment of peptide orientation in lipid vesicle membrane, Proc. Natl. Acad. Sci. USA 99 (2002) 15313–15317.
[50] P.J. Wyatt, Cell wall thickness, Size distribution, refractive index ratio and dry weight content of living bacteria, Nature 226 (1970) 277–279.